Journal of Solid Mechanics Vol. 9, No. 2 (2017) pp. 396-410

Static and Free Vibration Analyses of Orthotropic FGM Plates Resting on Two-Parameter Elastic Foundation by a Mesh-Free Method

H. Momeni-Khabisi *

Department of Mechanical Engineering, University of Jiroft , Jiroft , Iran

Received 18 March 2017; accepted 14 May 2017

ABSTRACT

In this paper, static and free vibrations behaviors of the orthotropic functionally graded material (FGM) plates resting on the two-parameter elastic foundation are analyzed by the a mesh-free method based on the first order shear deformation plate theory (FSDT). The mesh-free method is based on moving least squares (MLS) shape functions and essential boundary conditions are imposed by transfer function method. The orthotropic FGM plates are made of two orthotropic materials and their volume fractions are varied smoothly along the plate thickness. The convergence of the method is demonstrated and to validate the results, comparisons are made with finite element method (FEM) and the others available solutions for both homogeneous and FGM plates then numerical examples are provided to investigate the effects of material distributions, elastic foundation coefficients, geometrical dimensions, applied force and boundary conditions on the static and vibrational characteristics of the orthotropic FGM plates.

Keywords : Static; Free vibration; FGM plate; Orthotropic; Mesh-free.

1 INTRODUCTION

FUNCTIONALLY graded materials are classified as novel composite materials with gradient compositional variation. This effect can be alleviated by functionally grading the material to have a smooth spatial variation of material composition, with ceramic-rich material and metal-rich material in regions where mechanical properties, such as toughness, need to be high. Therefore FGMs have a non-uniform microstructure and a continuously variable macrostructure. FGMs are widely used in many structural applications such as aerospace, energy conversion, nuclear, civil, heat generators and automotive because of their high performance of heat resistant [1]. They may also be supported by an elastic foundation. These kinds of plates are mainly used in concrete roads, raft, and mat foundations of buildings and reinforced concrete pavements of airport runways. To describe the interaction between plate and foundation, various kinds of foundation models have been proposed. The simple stone is Winkler or one-parameter model which regards the foundation as a series of separated spring without coupling effects between each other. This model was improved by Pasternak by adding a shear spring to simulate the interactions between the separated springs in the Winkler model. The Pasternak or two-parameter model is widely used to describe the mechanical behavior of structure-foundation interactions [2].

Several numerical and analytical solutions have been presented for the analysis of FG plates. The classical plate theory (CPT), which neglects the transverse shear deformation effect, provides reasonable results for thin plate. It

*Corresponding author. Tel.: +98 344 3347061.
E-mail address: h.momeni@ujiroft.ac.ir (H. Momeni-Khabisi).

underestimates deflections and overestimates frequencies as well as buckling loads of moderately thick plate [3]. So, many shear deformation plate theories which account for the transverse shear deformation effect have been developed for overcoming on the limitation of CPT. The Reissner [4] and Mindlin [5] theories are known as first order shear deformation plate theory. FSDT provides a sufficiently accurate description of response for thin to moderately thick plate [6]. The performance of the FSDT is strongly dependent on shear correction factors which are sensitive not only to the material and geometric properties but to the loading and boundary conditions. To avoid the use of shear correction factor and to include the actual cross-section warping of the plate, higher-order shear deformation theories (HSDTs) have been extensively developed, considering the higher-order variation of in-plane displacement through the thickness [7]. Matsunaga [8] presented natural frequencies and buckling stresses of FGM plates by taking into account the effects of transverse shear and normal deformations and rotatory inertia based on two-dimensional (2-D) higher-order theory.

Malekzadeh [9] studied free vibration analysis of thick FG plates supported on two-parameter elastic foundations by using Differential Quadrature (DQ) method and based on the three-dimensional elasticity theory. Elasticity solution for free vibrations analysis of functionally graded fiber reinforced plates on elastic foundation was studied by Yas and Sobhani [10]. Ferreira et al. [11] presented static deformations and free vibrations of shear flexible isotropic and laminated composite plates with a FSDT theory based on a high order collocation method. They also analyzed isotropic and laminated plates by Kansa's non-symmetric radial basis function collocation method based on a HSDT [12]. Nie and Batra [13] presented static deformations of FG polar-orthotropic cylinders with elliptical inner and circular outer surfaces. Zhang et al. [14] presented nonlinear dynamics and chaos of a simply supported orthotropic FGM rectangular plate in thermal environment and subjected to parametric and external excitations based on the Reddy's third-order shear deformation plate theory and Galerkin procedure. The free vibration analysis of initially stressed thick simply supported functionally graded curved panel resting on two-parameter elastic foundation, subjected in thermal environment is studied using the three-dimensional elasticity formulation by Farid et al. [15]. Thai and Choi [2,6] developed a refined plate theory for free vibration and buckling analyses of FGM plates resting on elastic foundation. Zhu et al. [16] studied on bending and free vibration analyses of thin-to-moderately thick functionally graded carbon nanotube-reinforced composite (FG-CNTRC) plates using the FEM based on the FSDT plate theory. Jam et al. [17] focused on free vibration characteristics of rectangular FGM plates resting on Pasternak foundation based on the three-dimensional elasticity theory and by means of the generalized DQM. Alibeigloo and Liew [18] presented bending behavior of FG-CNTRC rectangular plate with simply supported edges subjected to thermo-mechanical loads based on three-dimensional theory of elasticity. Asemi and Shariyat [19] developed a highly accurate nonlinear three-dimensional energy-based finite element elasticity formulation for buckling investigation of anisotropic FGM plates with arbitrary orthotropy directions. They used a full compatible Hermitian element with 168 degrees of freedom, which satisfies continuity of the strain and stress components at the mutual edges and nodes of the element a priori to achieve most accurate results. Mansouri and Shariyat [20] investigated on the thermal buckling of the orthotropic FGM plates. They considered the effects of the bending-extension-shear coupling and pre-buckling by using a DQ method. They also presented thermo-mechanical buckling analysis of the orthotropic auxetic plates (with negative Poisson ratios) in the hygrothermal environments and resting on an elastic foundation [21]. Shariyat and Asemi [22] used a non-linear FEM and three-dimensional elasticity theory to investigate shear buckling of the orthotropic heterogeneous FGM plates resting on Winkler elastic foundation. Sofiyev et al. [23] presented analytical formulations and solutions for the stability analysis of heterogeneous orthotropic truncated conical shell subjected to external (lateral and hydrostatic) pressures with mixed boundary conditions using the Donnell shell theory. Moradi-Dastjerdi et al. [24] studied on the free vibration analysis of FG-CNTRC sandwich plates resting on two-parameter elastic foundation by a refined plate theory and Navier's method.

Some forms of mesh-free method were also used to analysis of FGM structures. Static, free vibration, dynamic and stress wave propagation analysis of FGM cylinders are presented by the same mesh-free method which used in this paper [25-27]. But in these work, structures are isotropic and axisymmetric cylinders. Moradi-Dastjerdi et al. [28] studied free vibration analysis of orthotropic FGM cylinders by the same mesh-free method. Dinis et al. [29] presented a three-dimensional shell-like approach for the analysis of isotropic and orthotropic thin plates and shells using natural neighbour radial point interpolation method which is a kind of mesh-free method based on radial basis function. Rezaei Mojdehi et al. [30] presented three dimensional (3D) static and dynamic analysis of thick isotropic FGM plates based on the Meshless Local Petrov–Galerkin (MLPG) which is used 3D-MLS shape functions. Lei et al. [31-32] studied buckling and free vibration analyses of FG-CNTRC plates, using the element-free *kp*-Ritz method based on FSDT. But in an absorbing work, Yaghoubshahi and Alinia [33] developed Element Free Galerkin (EFG) method based on HSDT to eliminate transverse shear locking in analysis of laminated composite plates and compared their results with those obtained by EFG procedure based on FSDT. Finally in two near works, Zhang et

al. [34-35] proposed an element-free based improved moving least squares-Ritz (IMLS-Ritz) method and FSDT to study the buckling behavior of FG-CNTRC plates resting on Winkler foundations and nonlinear bending of these plates resting on two-parameter elastic foundation.

It can be seen that static and free vibration analyses of the orthotropic FGM plates (made of two orthotropic materials) have not been investigated in past studies. So, in this paper, based on the first order shear deformation plate theory, a mesh-free method is developed to investigate static and free vibration characteristics of the orthotropic FGM plates resting on two-parameter elastic foundation. In the mesh-free method, MLS shape functions are used for approximation of displacement field in the weak form of motion equation and the transformation method is used for imposition of essential boundary conditions. This mesh-free method does not increase the calculations against EFG [28]. The orthotropic FGM plates are assumed to be composed of two orthotropic materials and their volume fractions are varied smoothly along the plate thickness. The influences of Pasternak's elastic foundation coefficients on the static and free vibrational behaviors of the orthotropic FGM plates are examined. The effects of material distributions, plate thickness-to-width ratio, plate aspect ratio, applied force and boundary conditions are also examined.

2 MATERIAL PROPERTIES IN ORTHOTROPIC FGM PLATES

Consider an orthotropic plate of length a, width b, thickness h, with an arbitrary combination of boundary conditions along the four edges, as shown in Fig. 1. Material properties of the plate are assumed to be graded along the thickness. The profile of this variation has important effects on the plate behavior. Several models have been proposed for variation of material properties. Among these models, volume fraction model is used more than other models. In this model, material properties of plate are varied as follows [2]:

$$P(z) = P_b + (P_t - P_b)(\frac{1}{2} + \frac{z}{h})^n \tag{1}$$

where P is an indicator for material properties of plate that is used instead of modulus elasticity, E, Poisson's ratio, υ, and density, ρ. Also, the subscripts b and t represent the bottom and top constituents, respectively; and n is the volume fraction exponent. The value of n equal to zero represents a homogeneous plate made of top constituents, whereas infinite n indicates a homogeneous plate made of bottom constituents.

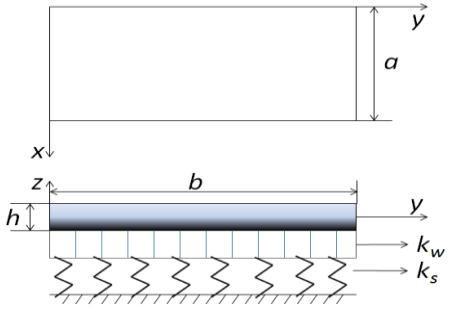

Fig.1
Schematic of FGM plate resting on two-parameter elastic foundation.

3 GOVERNING EQUATIONS

Based on the FSDT, the displacement components can be defined as [35]:

$$\begin{aligned} u(x,y,z) &= u_0(x,y) + z\,\theta_x(x,y) \\ v(x,y,z) &= v_0(x,y) + z\,\theta_y(x,y) \\ w(x,y,z) &= w_0(x,y) \end{aligned} \tag{2}$$

where u, v and w are displacements in the x, y, z directions, respectively. u_0, v_0 and w_0 denote midplane displacements, θ_x and θ_y rotations of normal to the midplane about y-axis and x-axis, respectively. The kinematic relations can be obtained as follows [35]:

$$\begin{bmatrix}\varepsilon_{xx} & \varepsilon_{yy} & \gamma_{xy}\end{bmatrix}^T = \varepsilon_0 + zk \ , \ \begin{bmatrix}\gamma_{yz} & \gamma_{xz}\end{bmatrix}^T = \gamma_0 \tag{3}$$

where:

$$\varepsilon_0 = \begin{Bmatrix} \partial u_0/\partial x \\ \partial v_0/\partial y \\ \partial u_0/\partial y + \partial v_0/\partial x \end{Bmatrix}, k = \begin{Bmatrix} \partial \theta_x/\partial x \\ \partial \theta_y/\partial y \\ \partial \theta_x/\partial y + \partial \theta_y/\partial x \end{Bmatrix}, \gamma_0 = \begin{Bmatrix} \partial v/\partial z + \partial w/\partial y \\ \partial u/\partial z + \partial w/\partial x \end{Bmatrix} = \begin{Bmatrix} \phi_y + \partial w_0/\partial y \\ \phi_x + \partial w_0/\partial x \end{Bmatrix} \tag{4}$$

The linear constitutive relations of a FG plate can be written as [36]:

$$\begin{Bmatrix}\sigma_x \\ \sigma_y \\ \sigma_{xy}\end{Bmatrix} = \begin{bmatrix} Q_{11}(z) & Q_{12}(z) & 0 \\ Q_{12}(z) & Q_{22}(z) & 0 \\ 0 & 0 & Q_{66}(z) \end{bmatrix} \begin{Bmatrix}\varepsilon_x \\ \varepsilon_y \\ \varepsilon_{xy}\end{Bmatrix} or \ \sigma = Q_b \varepsilon$$
$$\begin{Bmatrix}\sigma_{yz} \\ \sigma_{xz}\end{Bmatrix} = \alpha(z) \begin{bmatrix} Q_{44}(z) & 0 \\ 0 & Q_{55}(z) \end{bmatrix} \begin{Bmatrix}\varepsilon_{yz} \\ \varepsilon_{xz}\end{Bmatrix} or \ \tau = \alpha(z) Q_s \gamma \tag{5}$$

In which α denotes the transverse shear correction coefficient, which is suggested as $\alpha = 5/6$ for homogeneous materials and $\alpha = 5/(6-(\upsilon_{12t}(z)V_t(z) + \upsilon_{12b}(z)V_b(z)))$ for FGMs where $V_t = (1/2 + z/h)^n$ and $V_b = 1 - V_t$ denote volume fraction of materials [36]. Also where:

$$\begin{aligned} &Q_{11} = \frac{1-\nu_{23}(z)\nu_{32}(z)}{E_2(z)E_3(z)\Delta(z)}, Q_{22} = \frac{1-\nu_{31}(z)\nu_{13}(z)}{E_1(z)E_3(z)\Delta(z)}, Q_{12} = \frac{\nu_{21}(z)+\nu_{31}(z)\nu_{23}(z)}{E_2(z)E_3(z)\Delta(z)} \\ &Q_{44} = G_{23}(z), \ Q_{55} = G_{31}(z), \ Q_{66} = G_{12}(z) \\ &\Delta = \frac{1-\nu_{32}(z)\nu_{23}(z)-\nu_{21}(z)\nu_{12}(z)-\nu_{13}(z)\nu_{31}(z)-2\nu_{32}(z)\nu_{21}(z)\nu_{13}(z)}{E_1(z)E_2(z)E_3(z)} \end{aligned} \tag{6}$$

Also by considering of the Pasternak foundation model, total energy of the plate is as [2]:

$$U = \frac{1}{2}\int_V \left[\varepsilon^T \sigma + \gamma^T \tau - \rho(z)(\dot{u}^2 + \dot{v}^2 + \dot{w}^2)\right] dV + \frac{1}{2}\int_A \left[k_w w^2 + k_s \left[\left(\frac{\partial w}{\partial x}\right)^2 + \left(\frac{\partial w}{\partial y}\right)^2 \right] \right] dA + \int_A [qw] dA \tag{7}$$

where q is the applied load, k_w and k_s are coefficients of Winkler and Pasternak foundation. If the foundation is modeled as the linear Winkler foundation, the coefficient k_s in Eq. (7) is zero.

4 MESH-FREE NUMERICAL ANALYSIS

In these analyses moving least square shape functions introduced by Lancaster and Salkauskas [37] is used for

approximation of displacement vector in the weak form of motion equation. Displacement vector u can be approximated by MLS shape functions as follows [26]:

$$\hat{\mathrm{d}} = \sum_{i=1}^{N} \phi_i d_i \tag{8}$$

where N is the total number of nodes, $\hat{\mathrm{d}}$ is virtual nodal values vector and ϕ_i is MLS shape function of node located at $X(x, y) = X_i$ and they are defined as follows:

$$\hat{\mathrm{d}} = \left[\hat{u}_i, \hat{v}_i, \hat{w}_i, \hat{\theta}_x, \hat{\theta}_y\right]^T \tag{9}$$

and

$$\phi_i(\mathrm{X}) = \underbrace{\mathrm{P}^{\mathrm{T}}(\mathrm{X})\left[\mathrm{H}(\mathrm{X})\right]^{-1} W(\mathrm{X}-\mathrm{X}_i)\mathrm{P}(\mathrm{X}_i)}_{(1\times 1)} \tag{10}$$

In the above equation, W is cubic Spline weight function, P is base vector and H is moment matrix and are defined as follows:

$$\mathrm{P}(\mathrm{X}) = [1, x, y]^T \tag{11}$$

$$\mathrm{H}(\mathrm{X}) = \left[\sum_{i=1}^{n} W(\mathrm{X}-\mathrm{X}_i)\mathrm{P}(\mathrm{X}_i)\mathrm{P}^{\mathrm{T}}(\mathrm{X}_i)\right] \tag{12}$$

By using of the MLS shape function, Eq. (3) can be written as:

$$\varepsilon = \mathrm{B}_m \hat{\mathrm{d}} + z\mathrm{B}_b \hat{\mathrm{d}} \quad , \quad \gamma = \mathrm{B}_s \hat{\mathrm{d}} \tag{13}$$

In which [30]:

$$\mathrm{B}_m = \begin{bmatrix} \phi_{i,x} & 0 & 0 & 0 & 0 \\ 0 & \phi_{i,y} & 0 & 0 & 0 \\ \phi_{i,y} & \phi_{i,x} & 0 & 0 & 0 \end{bmatrix}, \mathrm{B}_b = \begin{bmatrix} 0 & 0 & 0 & \phi_{i,x} & 0 \\ 0 & 0 & 0 & 0 & \phi_{i,y} \\ 0 & 0 & 0 & \phi_{i,y} & \phi_{i,x} \end{bmatrix}, \mathrm{B}_s = \begin{bmatrix} 0 & 0 & \phi_{i,x} & \phi_i & 0 \\ 0 & 0 & \phi_{i,y} & 0 & \phi_i \end{bmatrix} \tag{14}$$

For elastic foundation, φ_w and B_p can be also defined as following:

$$\varphi_w = \begin{bmatrix} 0 & 0 & \phi_i & 0 & 0 \end{bmatrix}, \mathrm{B}_p = \begin{bmatrix} 0 & 0 & \phi_{i,x} & 0 & 0 \\ 0 & 0 & \phi_{i,y} & 0 & 0 \end{bmatrix} \tag{15}$$

Substitution of Eqs.(5) and (13) in Eq. (7) leads to:

$$U = \frac{1}{2}\int_A \hat{\mathrm{d}}\int_z \left[\mathrm{B}_m^T \mathrm{AB}_m + \mathrm{B}_m^T \bar{\mathrm{B}}\mathrm{B}_b + \mathrm{B}_b^T \bar{\mathrm{B}}\mathrm{B}_m + \mathrm{B}_b^T \mathrm{DB}_b + \mathrm{B}_s^T \mathrm{A}_s \mathrm{B}_s\right] dz\hat{\mathrm{d}}dA$$
$$-\frac{1}{2}\int_A \ddot{\hat{\mathrm{d}}}\int_z \left[\mathrm{G}_i^T \bar{\mathrm{M}}\mathrm{G}_j\right] dz\ddot{\hat{\mathrm{d}}}dA + \frac{1}{2}\int_A \left[\varphi_w^T k_w \varphi_w + \mathrm{B}_p^T k_s \mathrm{B}_p\right]\hat{\mathrm{d}}dA + \frac{1}{2}\int_A \varphi_w^T q dA \tag{16}$$

In which the components of the extensional stiffness A, bending-extensional coupling stiffness $\bar{\mathrm{B}}$, bending stiffness D, transverse shear stiffness A_s and also G_i and $\bar{\mathrm{M}}$ are introduced for mass matrix and they are defined as [32]:

$$(\mathrm{A}, \bar{\mathrm{B}}, \mathrm{D}) = \int_{-h/2}^{h/2} \mathrm{Q}_b (1, z, z^2) dz \quad , \quad \mathrm{A}_s = \alpha \int_{-h/2}^{h/2} \mathrm{Q}_s dz \tag{17}$$

and

$$\mathrm{G}_i = \begin{bmatrix} \phi_i & 0 & 0 & 0 & 0 \\ 0 & \phi_i & 0 & 0 & 0 \\ 0 & 0 & \phi_i & 0 & 0 \\ 0 & 0 & 0 & \phi_i & 0 \\ 0 & 0 & 0 & 0 & \phi_i \end{bmatrix}, \quad \bar{\mathrm{M}} = \begin{bmatrix} I_0 & 0 & 0 & I_1 & 0 \\ 0 & I_0 & 0 & 0 & I_1 \\ 0 & 0 & I_0 & 0 & 0 \\ I_1 & 0 & 0 & I_2 & 0 \\ 0 & I_1 & 0 & 0 & I_2 \end{bmatrix} \tag{18}$$

where I_0, I_1 and I_2 are the normal, coupled normal-rotary and rotary inertial coefficients, respectively and defined by:

$$(I_0, I_1, I_2) = \int_{-h/2}^{h/2} \rho(z)(1, z, z^2) dz \tag{19}$$

It can be noticed that the arrays of bending-extensional coupling stiffness matrix, $\bar{\mathrm{B}}$, are zero for symmetric laminated composites. Finally, by a derivative with respect to displacement vector, $\hat{\mathrm{d}}$, the Eq. (16) can be expressed as:

$$\mathrm{M}\ddot{\hat{\mathrm{d}}} + \mathrm{K}\hat{\mathrm{d}} = \mathrm{F} \tag{20}$$

In which, *M, K* and *F* are mass matrix, stiffness matrix and force vector, respectively and are defined as:

$$\mathrm{M} = \int_A \mathrm{G}_i^T \bar{\mathrm{M}}\mathrm{G}_j dA \tag{21}$$

$$K = K_m + K_b + K_s + K_w + K_p \tag{22}$$

$$\mathrm{F} = \int_A \varphi_w^T q dA \tag{23}$$

In which, K_m, K_b and K_s are stiffness matrixes of extensional, bending-extensional and bending, respectively and also, K_w and K_p are stiffness matrixes that represented the Winkler and Pasternak elastic foundations. They are defined as:

$$K_m = \int_A \left[\mathrm{B}_m^T \mathrm{A} \mathrm{B}_m + \mathrm{B}_m^T \bar{\mathrm{B}} \mathrm{B}_b + \mathrm{B}_b^T \bar{\mathrm{B}} \mathrm{B}_m \right] dA \ , \ K_b = \int_A \mathrm{B}_b^T \mathrm{D} \mathrm{B}_b dA \ , \ K_s = \int_z \mathrm{B}_s^T \mathrm{A}_s \mathrm{B}_s dA \tag{24}$$

$$K_w = \int_A \varphi_w^T k_w \varphi_w dA \ , \ K_p = \int_A \mathrm{B}_p^T k_s \mathrm{B}_p dA \tag{25}$$

For numerical integration, problem domain is discretized to a set of background cells with gauss points inside each cell. Then global stiffness matrix K is obtained numerically by sweeping all gauss points.

Imposition of essential boundary conditions in the system of Eq. (20) is not possible. Because MLS shape functions do not satisfy the Kronecker delta property. In this work transformation method is used for imposition of essential boundary conditions. For this purpose transformation matrix is formed by establishing relation between nodal displacement vector $\mathbf{d}$ and virtual displacement vector $\hat{\mathrm{d}}$.

$$\mathrm{d} = \mathrm{T} \hat{\mathrm{d}} \tag{26}$$

T is the transformation matrix that is a ($5N$×$5N$) matrix and for each node is defined as [26]:

$$\mathrm{T}_i = \begin{bmatrix} \phi_i & \phi_i & \phi_i & \phi_i & \phi_i \\ \phi_i & \phi_i & \phi_i & \phi_i & \phi_i \\ \phi_i & \phi_i & \phi_i & \phi_i & \phi_i \\ \phi_i & \phi_i & \phi_i & \phi_i & \phi_i \\ \phi_i & \phi_i & \phi_i & \phi_i & \phi_i \end{bmatrix} \tag{27}$$

By using Eq. (26), system of linear Eq. (20) can be rearranged to:

$$\hat{\mathrm{M}} \ddot{\mathrm{d}} + \hat{\mathrm{K}} \mathrm{d} = \hat{\mathrm{F}} \tag{28}$$

where,

$$\hat{\mathrm{M}} = \mathrm{T}^{-T} \mathrm{M} \mathrm{T}^{-1} \ , \ \hat{\mathrm{K}} = \mathrm{T}^{-T} \mathrm{K} \mathrm{T}^{-1} \ , \ \hat{\mathrm{F}} = \mathrm{T}^{-T} \mathrm{F} \tag{29}$$

Now the essential B. Cs. can be enforced to the modified equations system (28) easily like the finite element method.

For static problem, the mass matrix is eliminated and Eq. (28) is changed to:

$$\hat{\mathrm{K}} \mathrm{d} = \hat{\mathrm{F}} \tag{30}$$

So, the stress and displacement fields of the plate can be derived by solving this equations system. In the absence of external forces, Eq. (28) is also simplified as follows:

$$\hat{\mathrm{M}} \ddot{\mathrm{d}} + \hat{\mathrm{K}} \mathrm{d} = 0 \tag{31}$$

So, natural frequencies and mode shapes of the plate are determined by solving this eigenvalue problem.

5 RESULTS AND DISCUSSIONS

In this section, the static and free vibration analyses are presented to investigate the mechanical characteristics of the orthotropic FGM plates by several numerical examples. The plates are assumed resting on two-parameter elastic foundation and the developed mesh-free method is used. At first, convergence and accuracy of the mesh-free

method on static and vibrational behaviours of the plates are examined by a comparison between the results and reported results in literatures. Then, new mesh-free results on the static and free vibration characteristics of the orthotropic FGM plates on the elastic foundation are reported. In the following simulations, material properties of the orthotropic FGM plates are assumed to vary from Glass-Epoxy at bottom to Graphite-Epoxy at top of the plate according to the Eq. (1). The material properties of Glass-Epoxy and Graphite-Epoxy are reported in Table 1. In all examples of orthotropic plates, the foundation parameters are also presented in the non-dimensional form of $K_w = k_w a^4 / D$ and $K_s = k_s a^2 / D$, in which $D = E_1 h^3 / 12(1-\upsilon_{12}{}^2)$ is a reference bending rigidity of the plate and is based on the mechanical properties of Graphite-Epoxy. The non-dimensional deflection and natural frequency of the orthotropic FGM plates are also based on the mechanical properties of Graphite-Epoxy and Glass-Epoxy, respectively and defined as [11]:

$$\bar{w} = 10 E_1 h^3 w \,/ q_0 a^4 \tag{32}$$

$$\hat{\omega} = \omega h \sqrt{\rho / E_1} \tag{33}$$

In which, q_0 is the value of applied (concentrated or uniformly distributed) load and w is central deflection.

Table 1
Mechanical properties of the applied orthotropic materials [38].

Materials	E_1 (GPa)	E_2 (GPa)	E_3 (GPa)	υ_{23}	υ_{31}	υ_{12}	G_{23} (GPa)	G_{31} (GPa)	G_{12} (GPa)	ρ (kg/m^3)
Graphite-Epoxy	155	12.1	12.1	0.458	0.248	0.248	3.2	4.4	4.4	1500
Glass-Epoxy	50	15.2	15.2	0.428	0.254	0.254	3.28	4.7	4.7	1800

5.1 Validation of models

In the first example, consider a simply supported homogeneous square plate under uniformly distributed load, q_0. In this example, the non-dimensional deflection of the plate is defined as $\hat{w} = 10^2 E h^3 w \,/ q_0 a^4$. The convergence of the developed mesh-free method in central non-dimensional deflection of the plate with $h/a = 0.02$ is shown in Fig. 2. It can be seen that the applied mesh-free method has very good convergence and agreement with exact results that are reported by Akhras et al. [39] in the bending analysis of plate. The deflections of this plate for various values of $h/a\,(= 0.1,\ 0.05,\ 0.02 \text{ and } 0.01)$ are also listed in Table 2. The accuracy of the applied method is evident by comparison with the exact [39] and the other reported results [11,12,40]. The figure and table results show that, by using of only 11×11 node arrangement, the applied method has more accuracy than FEM.

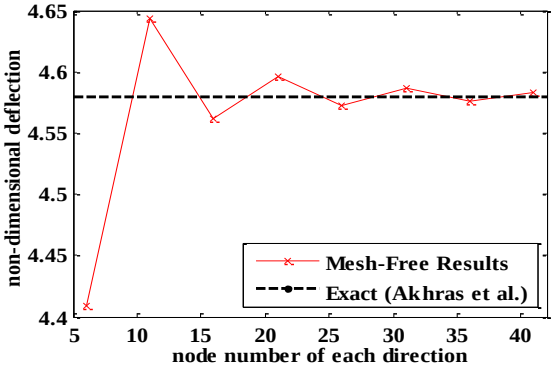

Fig.2
Convergence of the central non-dimensional deflection, $\hat{w}$, for different number of node in each direction.

In the second example of validation, consider a simply supported FGM square plate as Thai and Choi [2]. The convergence of the applied mesh-free method in non-dimensional fundamental frequency of the plates resting on Winkler-Pasternak elastic foundation with $h/a = 0.2, K_w = 100, K_s = 100$ and for two values of volume fraction exponent, $n = 0$ and $n = 1$, are shown in Figs. 3 and 4, respectively. This figure shows that, by using of only 5×5

node arrangement, the applied method has a very good accuracy and agreement with reported results by Thai and Choi [2] in homogenous ($n=0$) and FGM ($n=1$) plates. Also, the non-dimensional fundamental frequency of this plate are presented in Table 3. for various values of $h/a\left(=0.05,\ 0.1 \text{ and } 0.2\right)$ and elastic foundation coefficients. This table reveals that the applied method has very good accuracy and agreement with the reported results especially in thinner plates.

Table 2
Comparison of the central non-dimensional deflections, $\hat{w}$, in simply supported square plates subjected to uniformly distributed load.

h/a	Method	Non-dimensional Deflection
0.1	Present	4.7864
	Exact (Akhras et al. [39])	4.791
	Ferreira et al. 2003	4.7866
	Ferreira et al. 2009	4.7912
	FEM (Reddy [40])	4.770
0.05	Present	4.6274
	Exact (Akhras et al. [39])	4.625
	Ferreira et al. 2003	4.6132
	Ferreira et al. 2009	4.6254
	FEM (Reddy [40])	4.570
0.02	Present	4.5829
	Exact (Akhras et al. [39])	4.579
	Ferreira et al. 2003	4.5753
	Ferreira et al. 2009	4.5788
	FEM (Reddy [40])	4.496
0.01	Present	4.5765
	Exact (Akhras et al. [39])	4.572
	Ferreira et al. 2003	4.5737
	Ferreira et al. 2009	4.5716
	FEM (Reddy [40])	4.482

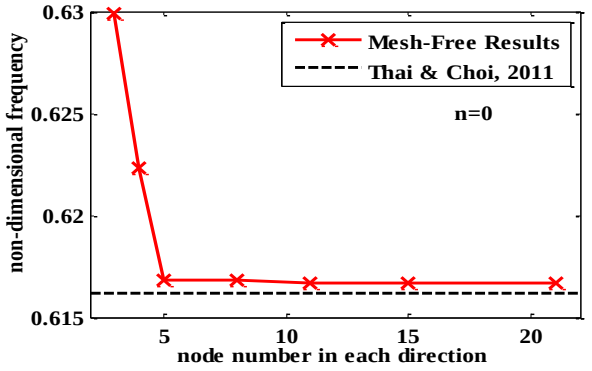

Fig.3
Convergence of the non-dimensional fundamental frequency, $\hat{\omega}$, of the FGM plate with n=0, h/a=0.2, K_w=100, K_s=100 for different number of node in each direction.

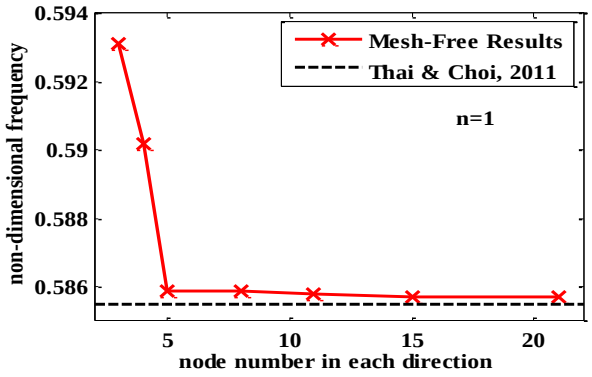

Fig.4
Convergence of the non-dimensional fundamental frequency, $\hat{\omega}$, of the FGM plate with n=1, h/a=0.2, K_w=100, K_s=100 for different number of node in each direction.

5.2 Static analysis of orthotropic FGM plates

At first, clamped square orthotropic FGM plates are considered. These plates are assumed under uniformly distributed load, q_0, and concentrated force, f_0, at the centre of plates with the same values. The central (maximum) non-dimensional deflections, $\bar{w}$, of the orthotropic FGM plates are listed in Table 4. for various values of volume fraction exponents, $n = 0,\ 0.1,\ 1,\ 10$ and 100, elastic foundation coefficients, K_w and $K_s = 0$ and 100, and ratio of thickness to length of plate, $h/a = 0.1$ and 0.2. This table reveals that, the concentrated forced is caused more deflection than uniformly distributed load. The elastic foundation decreases the deflection and the effect of Pasternak coefficient, K_s, on the deflection of plate is more than Winkler coefficient, K_w. Increasing of the thickness plate increases the non-dimensional deflections because of the $\bar{w}$ definition but the deflection is decreased by increasing of the thickness. But, the volume fraction exponent has an inverse manner in $h/a = 0.1$ and 0.2. In $h/a = 0.1$, increasing of *n* increases the deflection parameter (except in $n = 0$ for concentrated force), but in $h/a = 0.2$, this increasing, decreases (except in $n = 100$) the deflection parameter. So, the minimum deflections are occurred at $n = 0.1$ (for plates resting on elastic foundation) and $n = 10$ for the plates subjected the concentrated force with $h/a = 0.1$ and 0.2, respectively. For the orthotropic FGM plates under uniformly distributed load and with $h/a = 0.1$, minimum and maximum values of deflections are occurred at $n = 10$ (homogeneous plates made of fully Graphite-Epoxy) and $n = 100$, respectively.

Table 3
Comparison of the non-dimensional fundamental frequency, $\hat{\omega}$, in simply supported square FGM plates.

K_w	K_s	*h/a*	Method	*n*=0	*n*=1
0	0	0.05	Present	0.0291	0.0222
			Baferani et al. 2011	0.0291	0.0227
			Thai & Choi, 2011	0.0291	0.0222
		0.1	Present	0.1135	0.0869
			Baferani et al. 2011	0.1134	0.0891
			Thai & Choi, 2011	0.1135	0.0869
		0.2	Present	0.4167	0.3216
			Baferani et al. 2011	0.4154	0.3299
			Thai & Choi, 2011	0.4154	0.3207
100	100	0.05	Present	0.0411	0.0384
			Baferani et al. 2011	0.0411	0.0388
			Thai & Choi, 2011	0.0411	0.0384
		0.1	Present	0.1618	0.1519
			Baferani et al. 2011	0.1619	0.1542
			Thai & Choi, 2011	0.1619	0.1520
		0.2	Present	0.6167	0.5857
			Baferani et al. 2011	0.6162	0.5978
			Thai & Choi, 2011	0.6162	0.5855

Table 4
The central non-dimensional deflections, $\bar{w}$, in clamped square orthotropic FGM plates on elastic foundation.

Force kind	*h/a*	K_w	K_s	*n*				
				0	0.1	1	10	100
f_0	0.1	0	0	7.7010	7.7165	7.9937	8.2829	8.6221
			100	1.0707	1.0705	1.0712	1.0716	1.0736
		100	0	6.7835	6.7808	6.8895	6.9996	7.1542
			100	1.0605	1.0602	1.0608	1.0610	1.0628
	0.2	0	0	24.3850	24.2975	24.1432	24.0635	24.2839
			100	1.2106	1.2104	1.2098	1.2093	1.2096
		100	0	20.5518	20.4827	20.2699	20.0917	20.1324
			100	1.1990	1.1988	1.1982	1.1976	1.1979
q_0	0.1	0	0	0.7842	0.7959	0.8880	0.9798	1.0686
			100	0.0746	0.0747	0.0753	0.0758	0.0762
		100	0	0.5197	0.5254	0.5674	0.6064	0.6412
			100	0.0711	0.0711	0.0717	0.0722	0.0726

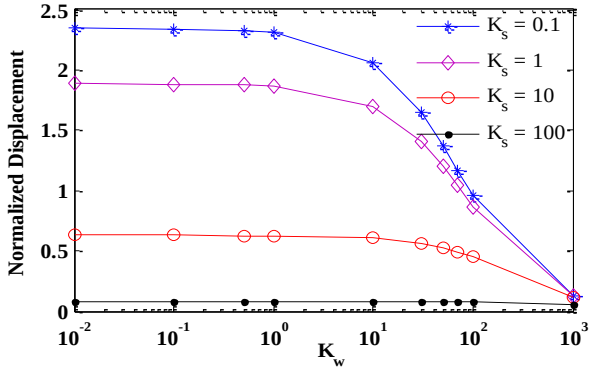

Fig.5
The central non-dimensional deflection, $\bar{w}$, versus Winkler coefficient for different Pasternak coefficient values.

To investigate the effect of elastic foundation coefficients, simply supported orthotropic FGM plates under uniformly distributed load are considered with $a/b=1, h/a=0.1$ and $n=1$. The plates are resting on two-parameter elastic foundation. Fig. 5 shows the central non-dimensional deflection, $\bar{w}$, of the plates versus Winkler (linear) coefficient, K_w , for various values of Pasternak (shear) coefficient, K_s ,. It can be seen that, the deflection of the plates is decreased by increasing of each coefficients of elastic foundation, especially for their values that are more than one. For values of $K_w > 1$, variation of K_s also has a big effect on the deflection of plates, but for $K_s = 100$, the variation of K_w has not an important effect on the deflection.

Consider clamped orthotropic FGM plates under uniformly distributed load resting on two-parameter elastic foundation to investigated stress distribution along the thickness. The plates are square and with $h/a=0.1, K_w=10$ and $K_s=100$. Figs. 6 show the stress distributions of, $\sigma_{xx}, \sigma_{yy}, \sigma_{xy}, \sigma_{xz}$ and σ_{yz} , along the thickness for various values of volume fraction exponent, $n=0,\ 0.1,\ 1$ and 10 at central point of the plate. These figures reveal that the values of normal stresses are so more than the values of shear stresses and the value of volume fraction exponent has significant effect on stress distributions.

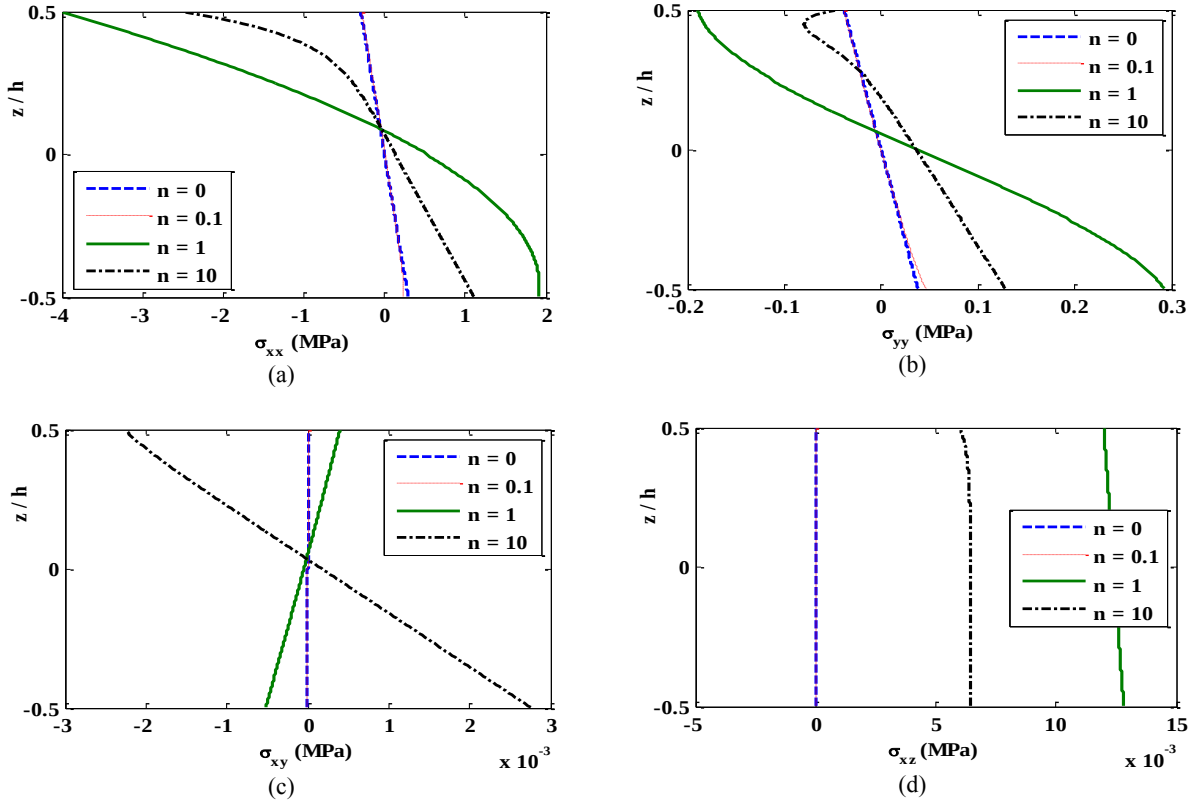

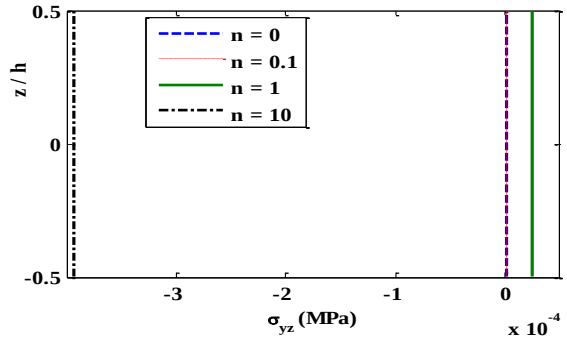

(e)

Fig.6

Stress distributions of, a) σ_{xx} b) σ_{yy} c) σ_{xy} d) σ_{xz} e) σ_{yz} , along the thickness at central point of the clamped orthotropic FGM plates under uniformly distributed load resting on the elastic foundation.

5.3 Free vibration analysis of orthotropic FGM plates

In the first example, the effects of elastic foundation coefficients, plate thickness and materials distribution are investigated on the vibrational behaviours of square orthotropic FGM plates. The non-dimensional fundamental frequencies of these square clamed plates are presented in Table 5. for various values of elastic foundation coefficients, K_w and $K_s = 0$ and 100, ratio of plate thickness, $h/a = 0.05$, 0.1 and 0.2, and volume fraction exponent, $n = 0$, 0.1, 1, 10 and 100. This table shows that increasing of the thickness plate increases the frequency parameter in the all cases. In most cases, increasing of the volume fraction exponent decreases the frequency parameter. Increasing in the values of elastic foundation coefficients also leads to increasing in frequency parameter in while Pasternak coefficient, K_s , has a bigger effect than the other one on the vibrational behaviours of the orthotropic FGM plates.

In the second example, the effects of boundary conditions and aspect ratio, a/b , are investigated on the vibrational behaviours of orthotropic FGM plates. Table 6. shows the non-dimensional fundamental frequencies, $\hat{\omega}$, for orthotropic FGM plates with $h/b = 0.1, K_w = 100, K_s = 10, a/b = 1$ and 3, various kinds of boundary conditions (*C* for Clamed, *F* for Free and *S* for simply supported edge)and for various values of *n*. It is evident that the frequency parameter is dramatically decreased by increasing in the ratio of a/b from 1 to 3 because the plate manners were nearing to beam manners. The clamped plate and free plate in all edges also have the biggest and the lowest values of frequency parameter, respectively. It can be seen that, CSCS and SSSS square plates almost have the same frequency parameter but in rectangular plate, the CSCS plate has higher frequency parameter values. Finally, increasing of the volume fraction exponent decreases the frequency parameter in the all cases because the fully Graphite-Epoxy plate is change to fully Glass-Epoxy plate.

Table 5

Non-dimensional fundamental frequency, $\hat{\omega}$, in clamped orthotropic FGM plates with *a*/*b*=1.

h/*a*	K_w	K_s	*n*				
			0	0.1	1	10	100
0.05	0	0	0.0285	0.0277	0.0239	0.0212	0.0198
		100	0.0713	0.0705	0.0669	0.0639	0.0631
	100	0	0.0319	0.0312	0.0276	0.0250	0.0237
		100	0.0727	0.0719	0.0682	0.0653	0.0644
0.1	0	0	0.0850	0.0837	0.0767	0.0707	0.0675
		100	0.2166	0.2166	0.2167	0.2169	0.2169
	100	0	0.1025	0.1011	0.0941	0.0882	0.0853
		100	0.2166	0.2166	0.2167	0.2169	0.2169
0.2	0	0	0.2122	0.2106	0.2016	0.1930	0.1888
		100	0.4331	0.4331	0.4333	0.4337	0.4337
	100	0	0.3119	0.3093	0.2969	0.2854	0.2816
		100	0.4331	0.4331	0.4333	0.4337	0.4337

Table 6
Non-dimensional fundamental frequency, $\hat{\omega}$, in orthotropic FGM plates with h/b=0.1, K_w=100, K_s=10.

B.Cs.	a/b	n				
		0	0.1	1	10	100
CCCC	1	0.1316	0.1301	0.1228	0.1166	0.1142
	3	0.0444	0.0443	0.0432	0.0422	0.0422
CCCS	1	0.1244	0.1230	0.1161	0.1105	0.1086
	3	0.0435	0.0434	0.0426	0.0418	0.0418
CCSS	1	0.1217	0.1202	0.1133	0.1077	0.1057
	3	0.0358	0.0357	0.0348	0.0340	0.0340
CSCS	1	0.1021	0.1015	0.0990	0.0968	0.0964
	3	0.0429	0.0429	0.0422	0.0414	0.0415
CCSF	1	0.0939	0.0931	0.0894	0.0862	0.0855
	3	0.0335	0.0334	0.0329	0.0323	0.0324
SSSS	1	0.1021	0.1015	0.0990	0.0968	0.0964
	3	0.0286	0.0285	0.0278	0.0271	0.0270
SSFF	1	0.0646	0.0642	0.0626	0.0612	0.0609
	3	0.0124	0.0123	0.0118	0.0114	0.0113
FFFF	1	0.0575	0.0570	0.0548	0.0529	0.0525
	3	0.0064	0.0063	0.0061	0.0059	0.0058

6 CONCLUSIONS

In this paper, static and free vibrations behaviors of the orthotropic FGM plates resting on the two-parameter elastic foundation were analyzed by the developed mesh-free method based on the first order shear deformation plate theory. The mesh-free method was based on MLS shape functions and essential boundary conditions were imposed by transfer function method. The orthotropic FGM plates were made of two orthotropic materials and their volume fractions were varied smoothly along the plate thickness.Numerical examples were provided to investigate the static and vibrational characteristics of the orthotropic FGM plates with different material distributions, elastic foundation coefficients, geometrical dimensions, applied force and boundary conditions. It is concluded that:

- The mesh-free method has a good convergence and accuracy in static and vibrational analyses of the orthotropic FGM plates and the method has more accuracy than FEM.
- The elastic foundation decreases deflection and increases fundamental frequency and also, the effect of shear coefficient is more than normal one.
- For high values of K_s, the variation of K_w has not an important effect on the deflection.
- Increasing of the plate thickness decreases deflection, but increases frequency of the plates.
- The volume fraction exponent has an inverse manner on the bending behaviour of the plates with various thicknesses but in most cases, increasing of the volume fraction exponent decreases the frequency parameter.
- The values of normal stresses are so more than the values of shear stresses and the value of volume fraction exponent has significant effect on stress distributions.
- The frequency parameter is dramatically decreased by increasing in the aspect ratio because the plate manners were nearing to beam manners.
- The essential boundary conditions have significant effect on the vibrational behaviors of the orthotropic FGM plate as the clamped plate and free plate in all edges have the biggest and the lowest values of frequency parameter, respectively.

REFERENCES

[1] Koizumi M., 1997, FGM activities in Japan, *Composites Part B* **28**: 1-4.
[2] Thai H.T., Choi D.H., 2011, A refined plate theory for functionally graded plates resting on elastic foundation, *Composites Science and Technology* **71**: 1850-1858.
[3] Reddy J.N., 2004, *Mechanics of Laminated Composite Plates and Shells: Theory and Analysis*, CRC.

[4] Reissner E., 1945, The effect of transverse shear deformation on the bending of elastic plates, *Journal of Applied Mechanics* **12**: 69-72.

[5] Mindlin R.D., 1951, Influence of rotatory inertia and shear on flexural motions of isotropic, elastic plates, *Journal of Applied Mechanics* **18**: 31-38.

[6] Thai H.T., Choi D.H., 2012, An efficient and simple refined theory for buckling analysis of functionally graded plates, *Applied Mathematical Modelling* **36**: 1008-1022.

[7] Reddy J. N., 1984, A simple higher order theory for laminated composite plates, *Journal of Applied Mechanics* **51**: 745-752.

[8] Matsunaga H., 2008, Free vibration and stability of functionally graded plates according to a 2-D higher-order deformation theory, *Composite Structures* **82**: 499-512.

[9] Malekzadeh P., 2009, Three-dimensional free vibration analysis of thick functionally graded plates on elastic foundations, *Composite Structures* **89**: 367-373.

[10] Yas M.H., Sobhani B., 2010, Free vibration analysis of continuous grading fibre reinforced plates on elastic foundation, *International Journal of Engineering Science* **48**: 1881-1895.

[11] Ferreira A.J.M., Castro L.M.S., Bertoluzza S., 2009, A high order collocation method for the static and vibration analysis of composite plates using a first-order theory, *Composite Structures* **89**: 424-432.

[12] Ferreira A.J.M., Roque C.M.C., Martins P.A.L.S., 2003, Analysis of composite plates using higher-order shear deformation theory and a finite point formulation based on the multiquadric radial basis function method, *Composites Part B* **34**: 627-636.

[13] Nie G.J., Batra R.C., 2010, Static deformations of functionally graded polar-orthotropic cylinders with elliptical inner and circular outer surfaces, *Composites Science and Technology* **70**: 450-457.

[14] Zhang W., Yang J., Hao Y., 2010, Chaotic vibrations of an orthotropic FGM rectangular plate based on third-order shear deformation theory, *Nonlinear Dynamic* **59**: 619-660.

[15] Farid M., Zahedinejad P., Malekzadeh P., 2010, Three-dimensional temperature dependent free vibration analysis of functionally graded material curved panels resting on two-parameter elastic foundation using a hybrid semi-analytic, differential quadrature method, *Materials and Design* **31**: 2-13.

[16] Zhu P., Lei Z.X., Liew K.M., 2012, Static and free vibration analyses of carbon nanotube-reinforced composite plates using finite element method with first order shear deformation plate theory, *Composite Structures* **94**: 1450-1460.

[17] Jam J.E., Kamarian S., Pourasghar A., Seidi J., 2012, Free vibrations of three-parameter functionally graded plates resting on pasternak foundations, *Journal of Solid Mechanics* **4**: 59-74.

[18] Alibeigloo A., Liew K.M., 2013, Thermoelastic analysis of functionally graded carbon nanotube-reinforced composite plate using theory of elasticity, *Composite Structures* **106**: 873-881.

[19] Asemi K., Shariyat M., 2013, Highly accurate nonlinear three-dimensional finite element elasticity approach for biaxial buckling of rectangular anisotropic FGM plates with general orthotropy directions, *Composite Structures* **106**: 235-249.

[20] Mansouri M.H., Shariyat M., 2014, Thermal buckling predictions of three types of high-order theories for the heterogeneous orthotropic plates, using the new version of DQM, *Composite Structures* **113**: 40-55.

[21] Mansouri M.H., Shariyat M., 2015, Biaxial thermo-mechanical buckling of orthotropic auxetic FGM plates with temperature and moisture dependent material properties on elastic foundations, *Composites Part B* **83**: 88-104.

[22] Shariyat M., Asemi K., 2014, Three-dimensional non-linear elasticity-based 3D cubic B-spline finite element shear buckling analysis of rectangular orthotropic FGM plates surrounded by elastic foundations, *Composites Part B* **56**: 934-947.

[23] Sofiyev A.H., Huseynov S.E., Ozyigit P., Isayev F.G., 2015, The effect of mixed boundary conditions on the stability behavior of heterogeneous orthotropic truncated conical shells, *Meccanica* **50**: 2153-2166.

[24] Moradi-Dastjerdi R., Payganeh Gh., Malek-Mohammadi H., 2015, Free vibration analyses of functionally graded CNT reinforced nanocomposite sandwich plates resting on elastic foundation, *Journal of Solid Mechanic* **7**: 158-172.

[25] Foroutan M., Moradi-Dastjerdi R., Sotoodeh-Bahreini R., 2012, Static analysis of FGM cylinders by a mesh-free method, *Steel and Composite Structures* **12**: 1-11.

[26] Mollarazi H.R., Foroutan M., Moradi-Dastjerdi R., 2012, Analysis of free vibration of functionally graded material (FGM) cylinders by a meshless method, *Journal of Composite Materials* **46**: 507-515.

[27] Foroutan M., Moradi-Dastjerdi R., 2011, Dynamic analysis of functionally graded material cylinders under an impact load by a mesh-free method, *Acta Mechanica* **219**: 281-290.

[28] Moradi-Dastjerdi R., Foroutan M., 2014, Free Vibration Analysis of Orthotropic FGM Cylinders by a Mesh-Free Method, *Journal of Solid Mechanics* **6**: 70-81.

[29] Dinis L.M.J.S., Natal Jorge R.M., Belinha J., 2010, A 3D shell-like approach using a natural neighbour meshless method: Isotropic and orthotropic thin structures, *Composite Structures* **92**:1132-1142.

[30] Rezaei Mojdehi A., Darvizeh A., Basti A., Rajabi H., 2011, Three dimensional static and dynamic analysis of thick functionally graded plates by the meshless local Petrov–Galerkin (MLPG) method, *Engineering Analysis with Boundary Elements* **35**: 1168-1180.

[31] Lei Z.X., Liew K.M., Yu J.L., 2013, Buckling analysis of functionally graded carbon nanotube-reinforced composite plates using the element-free kp-Ritz method, *Composite Structures* **98**:160-168.

[32] Lei Z.X., Liew K.M., Yu J.L., 2013, Free vibration analysis of functionally graded carbon nanotube-reinforced composite plates using the element-free kp-Ritz method in thermal environment, *Composite Structures* **106**:128-138.

[33] Yaghoubshahi M., Alinia M.M., 2015, Developing an element free method for higher order shear deformation analysis of plates, *Thin-Walled Structures* **94**: 225-233.
[34] Zhang L.W., Lei Z.X., Liew K.M., 2015, An element-free IMLS-Ritz framework for buckling analysis of FG–CNT reinforced composite thick plates resting on Winkler foundations, *Engineering Analysis with Boundary Elements* **58**: 7-17.
[35] Zhang L.W., Song Z.G., Liew K.M., 2015, Nonlinear bending analysis of FG-CNT reinforced composite thick plates resting on Pasternak foundations using the element-free IMLS-Ritz method, *Composite Structures* **128**: 165-175.
[36] Efraim E., Eisenberger M., 2007, Exact vibration analysis of variable thickness thick annular isotropic and FGM plates, *Journal of Sound and Vibration* **299**: 720-738.
[37] Lancaster P., Salkauskas K., 1981, Surface generated by moving least squares methods, *Mathematics of Computation* **37**: 141-158.
[38] Hyer M.W., 1998, *Mechanics of Composite Materials*, McGraw-Hill.
[39] Akhras G., Cheung M.S., Li W., 1994, Finite strip analysis for anisotropic laminated composite plates using higher-order deformation theory, *Composite Structures* **52**: 471-477.
[40] Reddy J.N., 1993, *Introduction to the Finite Element Method*, New York, McGraw-Hill.
[41] Baferani A.H., Saidi A.R., Ehteshami H.,2011, Accurate solution for free vibration analysis of functionally graded thick rectangular plates resting on elastic foundation, *Composite Structures* **93**: 1842-1853.